

See discussions, stats, and author profiles for this publication at: <https://www.researchgate.net/publication/260914118>

Microphase Mechanism of "Superquenching" of Luminescent Probes in Aqueous Solutions of DNA and Some Other Polyelectrolytes

ARTICLE in THE JOURNAL OF PHYSICAL CHEMISTRY B · MARCH 2014

Impact Factor: 3.3 · DOI: 10.1021/jp500713q · Source: PubMed

READS

24

5 AUTHORS, INCLUDING:



Michael Kuzmin

Lomonosov Moscow State University

59 PUBLICATIONS **593** CITATIONS

[SEE PROFILE](#)



Nikita Durandin

Russian Academy of Sciences

9 PUBLICATIONS **8** CITATIONS

[SEE PROFILE](#)



Vladimir Kuzmin

Russian Academy of Sciences

61 PUBLICATIONS **632** CITATIONS

[SEE PROFILE](#)

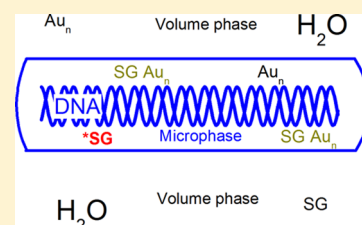
Microphase Mechanism of “Superquenching” of Luminescent Probes in Aqueous Solutions of DNA and Some Other Polyelectrolytes

Michael G. Kuzmin,^{*,†} Irina V. Soboleva,[†] Nikita A. Durandin,[‡] Ekaterina S. Lisitsyna,[‡] and Vladimir A. Kuzmin^{*,‡}

[†]Department of Chemistry, Moscow M. V. Lomonosov University, Leninskie Gory, Moscow 119991, Russia

[‡]N. M. Emanuel Institute of Biochemical Physics, Russian Academy of Sciences, Kosygin Street 4, Moscow 117997, Russia

ABSTRACT: A new approach in terms of microphase model of aqueous solutions of polyelectrolytes is proposed for explanation of a very strong quenching of luminescent probes (“superquenching”) in these solutions. This phenomenon is used in literature for creation of extremely sensitive chemical and biosensors and was attributed predominantly to efficient energy or electron transfer. Microphase approach considers this phenomenon in terms of local concentrations of both the luminescent compound and of the quencher in microphase, formed by DNA and other polyelectrolytes, which can be several (4–10) orders of magnitude greater than their apparent concentrations in solution. Large local concentrations of the light absorbing centers in the microphase also provide conditions for aggregation of these centers and efficient energy transfer, which provides a significant increase in quenching constants ($\sim 10^2$ – 10^5). Microphase approach provides good quantitative description of all the features of the superquenching, new possibilities for analysis and control of kinetics of DNA reactions, and for improvement of the sensitivity of luminescent sensors. It reveals nonspecific localization of the luminescent centers and of Au_n nanoparticles in different positions of DNA molecules that hinders from the simultaneous use of optical methods and electron or tunneling microscopy for the combined study of the structure of DNA.



INTRODUCTION

Very efficient quenching of luminescence of polyelectrolytes in aqueous solutions and in thin films by various electron or energy acceptors has been observed about a decade ago.^{1–13} This phenomenon, at which Stern–Volmer quenching constant exceeds 10^8 M^{-1} was called “superquenching”.^{1–4} Several applications of superquenching for development of extremely sensitive luminescent sensors were published.^{1–3,5–9,11–13} Originally, the behavior of superquenching was discussed in terms of an energy or exciton migration within the conjugated polymer chain to the quencher molecules, associated with polyelectrolyte.¹⁰

Recently, similar superquenching was observed in aqueous solutions of DNA, containing luminescent probes.¹⁴ In this case, small excitation energy ($<3 \text{ eV}$) and low local concentration of the probe prevent energy migration and it becomes clear that the mechanism of superquenching differs from the one proposed.

In this publication, we consider this phenomenon in terms of the microphase model of surfactant solutions, which was found to provide good quantitative description of the superquenching in various systems, using no special assumptions. Microphase approach provides useful tool for analysis of kinetics and mechanism of various reactions of DNA and for development of extremely sensitive analytical methods. Compartmental models of the reaction kinetics in micelles¹⁵ consider the effects of the distribution of the number of the quencher molecules between various microcompartments (micelles, vesicles, and so forth). In the case of the dynamic quenching

of the luminescent probe by some reactant molecules (a quencher Q), the rates of quenching $k_Q C_Q$ depend on the local concentrations of Q in the given compartments related to the distribution of the number of the quencher molecules between the compartments. When the rate of quenching is faster than the rate of the exchange by Q between compartments, one has to take into account the distribution of the number of the quencher molecules between compartments and the decay of the luminescent probe occurs to be nonexponential.

Microphase model considers different kind of microheterogeneous systems, where the rate of the exchange by the quencher between compartments is faster than the rate of the experiment (lifetime of the excited state in the case of dynamic quenching or time of the sample preparation in the case of the static quenching caused by ground-state complex formation). In this case, some average concentration C_Q in the microphase can be used and reaction kinetics follows the usual bimolecular or pseudounimolecular laws.

Microphase Model of Reactions in Microheterogeneous Solutions. Microphase (pseudophase) model considers aqueous solutions of surfactants (including micelles, vesicles, and so forth) as the two phase systems, containing volume phase (predominantly aqueous phase) and microphase (surfactant molecules together with counterions and reactant molecules).^{15–23} Local concentrations of the reactants inside

Received: January 21, 2014

Revised: February 27, 2014

the microphase can be several orders of magnitude greater than their apparent concentrations in the total solution. Main effects of this solubilization on the reaction kinetics are caused by the enhanced concentration of reactants as well as by local medium properties of the microphase. In contrast to the compartmental models that consider some distributions of the number of reactant molecules between the compartments of the microheterogeneous solution (that cause the distribution of the quenching rates and nonexponential decay of the luminescent probe) the microphase model implies some average concentration of the reactant in the microphase due to rather fast exchange of reactant molecules between the compartments.

The distribution of the reactants (a luminescent probe L and a quencher Q) between the microphase and volume phase can be described by ordinary distribution coefficients ρ_L and ρ_Q respectively

$$\rho_Q = \frac{[Q]_m}{[Q]_v} = \frac{C_{Qm}}{C_{Qv}} \quad (1)$$

where $[Q]_m$ and $[Q]_v$ (expressed in M) are the local concentrations of Q in microphase and in the volume phase, respectively, and $C_{Qm} = 0.6[Q]_m$ is the corresponding concentration expressed in molecules/nm³. Local concentration $[Q]_m$ depends on the apparent concentration $[Q]_0$ of Q in the total solution and the relative volume fraction of the microphase $v_m \approx M_{PRU}[PRU]_0/1000$ (where M_{PRU} and $[PRU]_0$ are molecular mass and molar concentration of the polymer repeat units in the total solution, respectively) as

$$[Q]_m = \rho_Q [Q]_v \approx \frac{[Q]_0}{v_m + \frac{1}{\rho_Q}} \quad (2)$$

or

$$C_{Qm} \approx \frac{0.6[Q]_0}{v_m + \frac{1}{\rho_Q}} \quad (3)$$

(at $v_m \ll 1$). Distribution coefficients ρ_L and ρ_Q depend on the hydrophobicity of the luminescent probe, quencher, and surfactant and their electric charges and can reach very large values ($10^5 - 10^{10}$).^{23,24} In such cases, local concentrations of L and Q can be many orders of magnitude greater than their apparent concentrations in the total solution and luminescence quenching can be caused either by formation of non-luminescent complexes between L and Q in the microphase or by nonstoichiometric interaction inside the quenching sphere with the volume V_Q . In both cases, the so-called static quenching can occur, when lifetime of the excited L^* remains constant and independent of $[Q]$.

Enhanced concentration of Q in the microphase can lead to the complex formation even at relatively small values of the equilibrium constants in the microphase



where subscripts m indicate that all reactants are localized in the microphase. Real equilibrium constant in the microphase $K_{Cm} = [LQ]_m/[L]_m[Q]_m = \exp(-\Delta G_{LQm}/RT)$ where ΔG_{LQm} is the free energy of the complex formation inside the microphase. In this case

$$\begin{aligned} \frac{\varphi}{\varphi_0} &= \frac{[L]_m}{[L]_{m0}} \\ &= 1 - \frac{1 + \frac{1}{K_{Cm}[L]_{m0}} + \frac{[Q]_{m0}}{[L]_{m0}}}{2} \\ &\quad + \left(\frac{\left(1 + \frac{1}{K_{Cm}[L]_{m0}} + \frac{[Q]_{m0}}{[L]_{m0}}\right)^2}{4} - \frac{[Q]_{m0}}{[L]_{m0}} \right)^{1/2} \\ &= 1 - \frac{1 + \frac{1}{K_{Cm}[L]_{m0}} + X}{2} \\ &\quad + \left(\frac{\left(1 + \frac{1}{K_{Cm}[L]_{m0}} + X\right)^2}{4} - X \right)^{1/2} \end{aligned} \quad (5)$$

where $X = [Q]_{m0}/[L]_{m0}$. Or, using the apparent concentrations $\alpha[L]_0$ and $[Q]_0$ in the total solution as the parameters

$$\begin{aligned} \frac{\varphi}{\varphi_0} &= 1 - \frac{1 + \frac{1}{K_Q\alpha[L]_0} + \frac{[Q]_0}{\alpha[L]_0}}{2} \\ &\quad + \left(\frac{\left(1 + \frac{1}{K_Q\alpha[L]_0} + \frac{[Q]_0}{\alpha[L]_0}\right)^2}{4} - \frac{[Q]_0}{\alpha[L]_0} \right)^{1/2} \end{aligned} \quad (6)$$

where $\alpha = (v_m + 1/\rho_Q)/(v_m + 1/\rho_L)$. Apparent quenching constant $K_Q = K_{Cm}/(v_m + 1/\rho_Q)$ can exceed actual K_{Cm} several orders of magnitude (since v_m reaches usually ca. 10^{-4} – 10^{-6} and $\rho_Q > 10^4$) and superquenching is observed. Apparent free energy of quenching $\Delta G_Q = -RT \ln K_Q = RT \ln((v_m + 1/\rho_Q)/K_{Cm}) = \Delta G_{Qm} + \Delta G_{Cm}$ is close to the sum of the solubilization energy of the quencher ΔG_{Qm} and actual free energy of the complex formation in the microphase ΔG_{Cm} .

When $[Q]_0 \gg [L]_0$ eq 5 is reduced to the well-known Stern–Volmer equation

$$\frac{\varphi}{\varphi_0} \approx \frac{1}{(1 + K_{SV}[Q])} \quad (7)$$

which provides apparent quenching constant $K_Q \approx K_{SV}$ (at $[Q] = [Q]_0 - [L]_0$). When $[Q]_0 \ll [L]_0$ eq 5 is reduced to

$$\frac{\varphi}{\varphi_0} \approx 1 - \frac{[Q]_0}{\alpha[L]_0} \quad (8)$$

which provides an estimation of the actual concentration of the luminescent centers in the system under investigation $[L]_0 \approx 1/K_{SV} ([Q] = [Q]_0 \text{ at } [Q]_0 \ll [L]_0)$. But at comparable $[L]_{0m}$ and $[Q]_{0m}$ the value of φ/φ_0 occurs to depend on the surfactant concentration v_m and $[L]_0$.

In the case of nonstoichiometric interaction between L and Q, the dependence of φ/φ_0 on C_{Qm} and $[Q]_0$ can be described by Perrin equation

$$\frac{\varphi}{\varphi_0} = \exp(-V_{Qm}C_{Qm}) \quad (9)$$

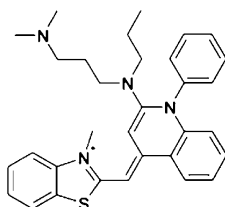
where V_{Qm} is the quenching volume (nm³) and C_{Qm} is a local quencher concentration in the microphase (molecules/nm³).

This equation formally corresponds to the definite radius of interaction between L and Q ($R_Q = (3/4\pi V_{Qm})^{1/3}$) or to the formation of infinite series of the complexes LQ_n with equal equilibrium constants $K = V_{Qm}$.

EXPERIMENTAL SECTION

Materials. Commercial aqueous solution of Derinat (ultrasonically depolymerized purified DNA from milt of sturgeon fishes, Na salt) with molecular mass $(0.25\text{--}0.5) \times 10^6$ Da was used in phosphate (10^{-2} M NaH_2PO_4) buffer containing 0.3 M NaCl (pH ~ 7.0). Concentration of DNA was determined spectrophotometrically, using $\epsilon_{260} \approx 6600 \text{ dm}^3 \text{ mole}^{-1} \text{ cm}^{-1}$.²⁵ Commercial dye SYBRGreen I (Sigma, U.S.A.) was used. SYBRGreen I is the trade name of the asymmetric cyanine dye (see Chart 1). Its concentration in solutions was controlled

Chart 1. Structure of SYBRGreen I



spectrophotometrically using $\epsilon_{494} = 73000 \text{ dm}^3 \text{ mole}^{-1} \text{ cm}^{-1}$.²⁶ Gold nanoparticles with average diameter ~ 2.5 nm were prepared in the form hydrosol by reduction of HAuCl_4 by tetrakis(hydroxymethyl)phosphonium chloride in aqueous solution.²⁷

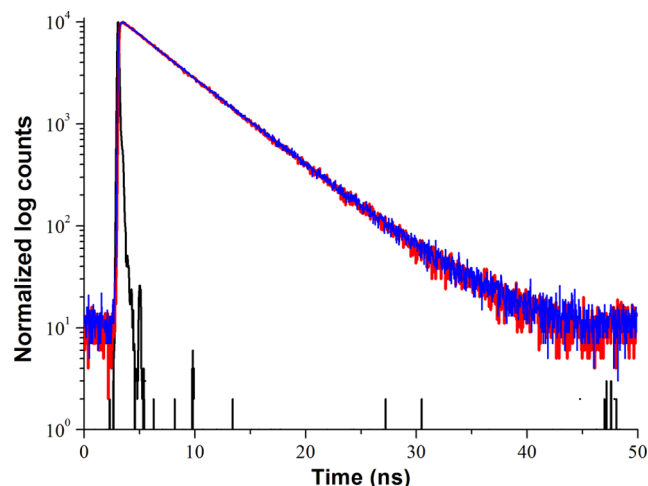


Figure 1. Normalized fluorescence decays at 525 nm for SG ($0.5 \mu\text{M}$) in aqueous solution of DNA ($30 \mu\text{M}$) in phosphate buffer for various concentration of Au nanoparticles (black, IRF; red, 0 M; blue, $0.2 \mu\text{M}$).

Table 1. SG Fluorescence Lifetime Measurements

[SG]/ μM	[DNA]/ μM (bp)	[Au]/ μM	τ/ns	χ^2
0.5	30	0	5.05	1.08
0.5	30	0.2	5.06	1.14

Steady State Spectroscopy. Absorption spectra were recorded with a Shimadzu UVVIS3101PC spectrophotometer in quartz cells 0.4×1.0 cm. Fluorescence spectra were

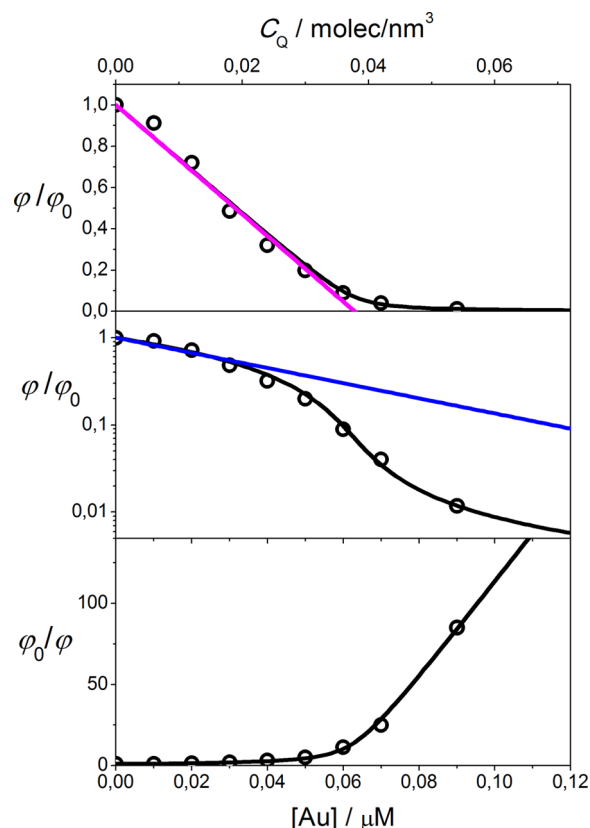


Figure 2. Dependence of relative fluorescence ($\lambda = 525$ nm) quantum yield ϕ/ϕ_0 (points) for SG ($0.3 \mu\text{M}$) in aqueous solution of DNA ($30 \mu\text{M}$) in phosphate buffer on the total concentration of Au_n nanoparticles in the solution (bottom axis) and local concentration in the microphase (top axis) in linear coordinates (top), semi-logarithmic coordinates (middle), and in Stern–Volmer coordinates (bottom). Black lines show the fitting of these data by eq 6 ($K_Q = 3000 \mu\text{M}^{-1}$, $\alpha[\text{SG}]_0 = 0.06 \mu\text{M}$); magenta line shows linear approximation (eq 8) at $[\text{Au}_n] < 0.1 \mu\text{M}$; blue line shows Perrin plot (eq 9, $V_Q = 20 \mu\text{M}^{-1} = 12 \text{ nm}^3/\text{molecule}$).

measured by Shimadzu 60RF5301PC spectrofluorimeter without a correction on detector sensitivity. The measurements were done in quartz cells 0.2×1.0 cm using $\lambda_{\text{Ex}} = 490$ nm and spectral widths of both slits 3 nm.

Fluorescence Lifetime Measurements. These measurements were performed by time-correlated single photon counting (TCSPC) method with a fluorescence steady state and lifetime spectrometer FluoTime 300 “EasyTau” (Picoquant GmbH, Germany) utilizing PicoHarp 300 TCSPC module and PDL 820 driver. Samples were excited in quartz cells 1.0×1.0 cm using laserhead LDH–P–C–485 $\lambda_{\text{Ex}} = 485 \pm 5$ and $\lambda_{\text{Reg}} = 525$ nm nm with τ_{Ex} (IRF) ~ 30 ps. The cutoff filter was used to neglect the influence of scattered excitation light. Signals were detected with microchannel plate photomultiplier tube (MCP–PMT) (R3809U–50 Hamamtsu). Data were fitted with exponential model with reconvolution by means of FluoFit software according to equation 10

$$I(t) = \int_{-\infty}^t \text{IRF}(t') \sum_{i=1}^n A_i e^{-t'/\tau_i} dt' \quad (10)$$

where A_i is the amplitude of the i_{th} component in counts at time zero; τ_i is the lifetime of the i_{th} component; and IRF is experimentally measured IRF (lamp function). The weighted

Table 2. Kinetic Parameters of the Luminescence Superquenching in Various Systems

luminescent probe		SYBRGreen		cyanine dye (pendant on each repeat unit of a synthetic poly(L-lysine)) ^a		poly(9,9-bis(6- <i>N,N,N</i> -trimethylammonium)-hexyl)-fluorene phenylene (PF) ^b	
quencher	Au _n (2 nm)			9,10-anthraquinone-2,6-disulfonate		Au _n (5 nm)	
medium	DNA in H ₂ O			Poly(L-lysine) in H ₂ O		PF in H ₂ O	
<i>n</i> _{PRU}	1000			33	250	~20	2
<i>M</i> _{PRU}	~330			~750	~750	~500	~500
[PRU] ₀ /μM	30			0.2	0.2	1	1
<i>ν</i> _m	10 ⁻⁵			~1.5 × 10 ⁻⁷	~1.5 × 10 ⁻⁷	0.5 × 10 ⁻⁶	
[L] ₀ /μM	0.035	0.1	0.3	0.2	0.2	1	
[Q] ₀	0.01–0.2 μM					0–120 pM	
[Q] _{1/2} /μM	0.015	0.03	0.07	0.023	0.0021	0.000012 (0.000009)	0.00017
<i>K</i> _{SV} /μM ⁻¹	8			43 **	480 **	83000	5800
(PRU/Q) ₅₀				6.8	92	85000	5900
α[L] ₀ /μM	0.03	0.06	0.14				
β[L] ₀ /μM				0.04	0.003	0.000012	
<i>K</i> _Q /μM ⁻¹	3000	3000	3000			270000	
<i>V</i> _Q /μM ⁻¹						48000	
<i>C</i> _{LM} /molec nm ⁻³	0.0018	0.0036	0.0084			1.3 × 10 ⁻⁷	
<i>K</i> _{QM} /α/nm ³ molec ⁻¹	5 × 10 ⁴	5 × 10 ⁴	5 × 10 ⁴			22 × 10 ⁶	
<i>V</i> _{QM} /nm ³ molec ⁻¹				(~9)	(~120)	4 × 10 ⁶	
<i>R</i> _Q /nm				(~1.3)	(~3)	~100	

^aAccording to the experimental data of ref 4. ^bAccording to the experimental data of ref 10.

mean-square deviation χ_2 was the criterion to evaluate quality of fit with acceptable $\chi_2 \leq 1.2$.

Fluorescence decays of SG in DNA microphase in the absence and in the presence of Au nanoparticles were recorded. Both these decays show monoexponential behavior with the constant lifetime of 5.05 ns corresponding to SG intercalated between DNA basepairs. It could be assumed that high local concentration of the quencher in microphase mediates a dynamic quenching that would lead to decreased lifetime. In case of micellar reactions, intracellular distribution of quencher should result in bi- or multiexponential decays due to multiexponential decays.¹⁵ As shown above, the presence of the quencher apparently does not affect fluorescence lifetime as well as decay behavior. Thus, it could be concluded that the nonfluorescent complex formation between dye and quencher in DNA microphase occurs in ground state.

RESULTS AND DISCUSSION

Quenching of SG Fluorescence in Solutions of DNA.

Quenching of fluorescence of SYBRGreen I (SG) by Au nanoparticles (2 nm) in aqueous solutions of DNA was studied since this luminescent probe has been widely used in biochemical assays, particularly for polymerase chain reaction test and nucleic acid detection.²⁸ Fluorescence quantum yield of SG in aqueous phase is very low ($\sim 10^{-4}$) and increases significantly (to ~ 0.1) in organic solvents or in complexes with target biomolecules (e.g., DNA). Two positive charges of SG were shown to facilitate the complex formation of the dye with DNA molecule²⁶ due to strong electrostatic interaction of the SG positive charges and negative charges of phosphate groups of nucleic acids. Furthermore, quinolin-thiazole part of the dye molecule intercalates into the DNA structure and saturated *N*-alkyl residues are disposed in the minor groove.²⁹ Extremely high values of the quenching constant ($K_Q = (\phi_0/\phi - 1)/[Q]_0 = 10^{10} - 10^{11} \text{ M}^{-1}$, where $[Q]_0$ is the total concentration of the quencher in solution) and deviations from Stern–Volmer

dependence were observed for superquenching of SG fluorescence by Au nanoparticles in aqueous solutions of DNA.³⁰

Strong quenching of SG fluorescence is observed in the presence of Au_n nanoparticles (0–0.3 μM) in the solution of DNA (30 μM) containing SG (0.1 μM) and phosphate buffer (10⁻² M NaH₂PO₄ + 0.3 M NaCl, pH = 7.0). Fluorescence intensity decreases during several minutes after addition of the solution of Au_n nanoparticles and reaches constant value after 5–10 min. But fluorescence decay lifetime remains the same as in the absence of the quencher (4.8 ns). This indicates typical static quenching, related to the formation of nonfluorescent complex or by nonstoichiometric interaction in the microphase. Slow decrease of the fluorescence intensity can be attributed to relatively slow solubilization of Au_n nanoparticles by the microphase of DNA.

An example of a plot of the relative fluorescence quantum yield ϕ/ϕ_0 on the total concentration of Au_n nanoparticles in solution is shown in Figure 2. The relative fluorescence quantum yield ϕ/ϕ_0 decreases linearly with $[Q]_0$, when $[Q]_0 < [L]_0$ with the slope $1/\alpha[L]_0 \approx 16 \mu\text{M}^{-1}$, which can be used for evaluation of $\alpha \approx 0.6$ (eq 8). Such a value of α indicates incomplete binding of Au_n nanoparticles in the microphase. The plot ϕ/ϕ_0 versus $[Q]_0$ has been fitted to eq 6, yielding values K_Q and $\alpha[L]_0$ shown in Table 2. The obtained value of K_{QM} (50 000 nm³/molecule = 83 000 M⁻¹) corresponds to the formation of weak complex LQ with $-\Delta G_{LQM} \approx 0.3 \text{ eV}$ in the microphase. Apparent $K_Q = \exp(-\Delta G_Q/RT)$ ($= 3 \times 10^9 \text{ M}^{-1}$) and $-\Delta G_{LQ} = RT \ln K_Q = 0.5 \text{ eV}$ are much larger since the latter includes the solubilization energy of Q in the microphase ($\sim -0.2 \text{ eV}$).

The plot ϕ_0/ϕ versus $[Q]_0$ shows strong deviations from Stern–Volmer equation since this equation is valid only at $[Q] > [L]_0$. Some other methods of linearization, used in literature in the case of stoichiometric complexes formation (for instance, Scatchard plot³¹ $(\phi/\phi_0)(1 - \phi/\phi_0) = (K_Q/K_{mC}[L]_{m0})[Q]_0(\phi/\phi_0)$

$\varphi_0) - 1/K_{\text{mC}}[L]_{\text{m0}})$ can lead to erroneous conclusions because of large scattering of the experimental points at $\varphi/\varphi_0 < 0.1$ and $\varphi/\varphi_0 > 0.9$.

Stoichiometric interaction of the luminescent probe and the quencher is confirmed also by the observed dependence of plots φ/φ_0 versus $[Q]_0$ on the concentration of the probe shown in the Figure 3. These dependences provide identical

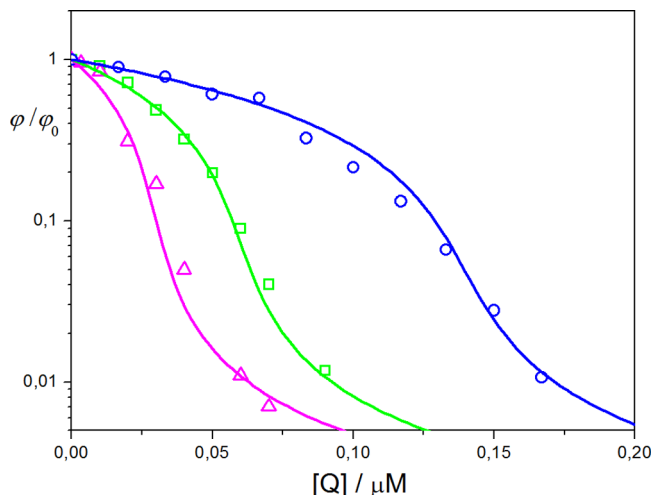


Figure 3. Dependences of relative fluorescence ($\lambda = 525$ nm) quantum yield φ/φ_0 (points) for SG in aqueous solution of DNA ($30 \mu\text{M}$) in phosphate buffer on the total concentration of Au_n nanoparticles in the solution for various total concentrations of SG (magenta triangles, $0.035 \mu\text{M}$; green squares, $0.1 \mu\text{M}$; blue circles, $0.3 \mu\text{M}$). Lines show the fitting with parameters given in the Table 2

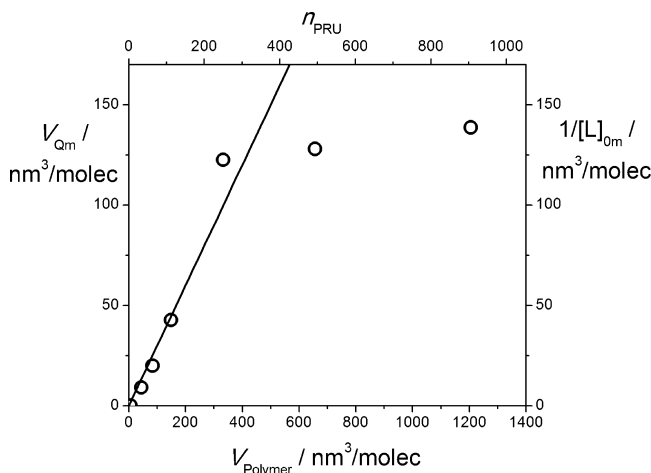


Figure 4. Dependence of Stern–Volmer quenching constants and quenching volume ($V_{\text{Qm}} \approx K_{\text{Qm}}$) in the microphase on the volume of poly(L-lysine) molecules, containing cyanine dye pendant on each repeat unit, for quenching by 9,10-anthraquinone-2,6-disulfonate in aqueous solutions.

values of K_{Q} at different $[L]_0$ and $\alpha[L]_0$ proportional to $[L]_0$ (see Table 2). All experimental plots φ/φ_0 versus $[Q]_0$ show substantial deviations from Perrin equation (eq 9), corresponding to nonstoichiometric interaction between L and Q. Thus, the observed quenching of SG fluorescence by Au_n nanoparticles in aqueous solutions of DNA, can be attributed to the formation of ground-state stoichiometric complex LQ in microphase.

Gradual decrease of SG fluorescence intensity during first 10 min after mixing of the solutions of SG and Au_n nanoparticles,¹⁴ indicates relatively slow increase of the local concentration of Au_n nanoparticles in the microphase of DNA. So slow kinetics of solubilization can be caused by Coulombic interaction of both negatively charged DNA phosphate groups and Au nanoparticles and corresponds to the activation energy ca. 0.6–0.7 eV.

Quenching of Fluorescence of Cyanine Dye Pendant on Polypeptide. Similar phenomena were described in the literature for aqueous solutions of some polyelectrolytes, containing luminescent centers, connected with each monomer unit,^{1–5} or included into the polymer chain.¹⁰ In these cases, the polymer can form the microphase, which already contains luminescent centers and their local concentration in the microphase does not depend on the concentration of the microphase. Quantitative relationships between relative fluorescence quantum yield and total quencher concentration in the solution were discussed in the literature in terms of Stern–Volmer quenching constants and in terms of an empirical parameter $(\text{PRU}/Q)_{50}$. Apparent $K_{\text{SV}} = (\varphi_0/\varphi - 1)/[Q]$ obtained from the experimental Stern–Volmer plots were found to be abnormally large ($K_{\text{SV}} \sim 10^6\text{--}10^9 \text{ M}^{-1}$) and depend on the concentration of polymer. Parameter $(\text{PRU}/Q)_{50}$ is equal to the ratio of the concentrations of polymer repeat unit (PRU) and quencher $[\text{PRU}]_0/[Q]_0$ at $\varphi/\varphi_0 = 0.5$ and does not depend on polymer concentration.

Whitten et al.⁴ studied quenching of fluorescence of polypeptides, containing cyanine dye pendant on each repeat unit of poly(L-lysines) with various number of PRU ($n_{\text{PRU}} = 5\text{--}900$) by 9,10-anthraquinone-2,6-disulfonate in aqueous solutions. It was shown that in diluted solutions of these polymers (with an optical density of ~ 0.05 at λ_{Max}) in the absence of the quencher an emission of J-aggregates is observed with biexponential decay kinetics. This kinetics indicates very fast energy transfer through the array of dye moieties from light absorbing centers to the luminescent centers (having some smaller excitation energy due to local microenvironment) and subsequent some slower (~ 60 ps) decay, which provides the dominant part of the measured steady-state emission intensity ($\varphi_0 \sim 0.01$). These data correspond to very efficient energy transfer to the luminescent centers with the emission rate constant $\sim 10^8 \text{ s}^{-1}$. One can use again eq 5 with parameter $1/K_{\text{Cm}}[L]_{\text{m0}}$ and variable $X = [Q]_{\text{m0}}/[L]_{\text{m0}} = [Q]_0/\beta[\text{PRU}]_0(\nu_{\text{m}} + 1/\rho_{\text{Q}})$.

To estimate the efficiency of the energy migration through the polymer molecule one can use some other parameter – an average number of quencher molecules per one polymer molecule necessary to quench a half of the luminescent centers

$$\left(\frac{[Q]}{[\text{Polymer}]} \right)_{1/2} = \frac{n_{\text{PRU}}[Q]_{1/2}}{[\text{PRU}]} = \frac{n_{\text{PRU}}}{\left(\frac{\text{PRU}}{Q} \right)_{50}} \quad (11)$$

The obtained values of $([Q]/[\text{Polymer}])_{1/2}$ were found to be ca. 2.6–4.4 for $n_{\text{PRU}} = 30\text{--}500$.⁴ This demonstrates directly that fast migration occurs through the whole array of dye moieties of the polymer molecule in this range of n_{PRU} . Only for long polymer chains with $n_{\text{PRU}} > 500$ this efficiency slightly decreases and $([Q]/[\text{Polymer}])_{1/2}$ reaches 9 that can be attributed to some hindrance, caused by defects in the polymer chain.⁴ Large value of $([Q]/[\text{Polymer}])_{1/2} = 30$, observed for oligomer with $n_{\text{PRU}} = 5$ and $([Q]/[\text{Polymer}])_{1/2} = 8000$ for monomer, can be

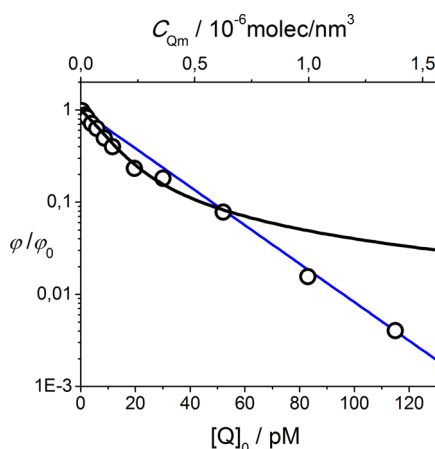


Figure 5. Experimental dependence of ϕ/ϕ_0 versus $[Q]_0$ (circles) for quenching of fluorescence of poly(9,9-bis(6-*N,N,N*-trimethylammonium)-hexyl)-fluorene-phenylene (PF) by Au_n nanoparticles (5 nm) (according to experimental data¹⁰ and its approximation by stoichiometric complex formation (black line, eq 6, $K_Q = 0.27 \text{ pM}^{-1}$, $\alpha[L]_0 = 12 \text{ pM}$) and by Perrin equation (blue line, eq 9, $V_{Qm} = 4 \times 10^6 \text{ nm}^3/\text{molecule}$).

attributed to weaker binding of the quencher by this oligomer and by the monomer.

It is not clear whether the stoichiometric complex is formed in these systems or nonstoichiometric quenching occurs, according to Perrin equation, because only the apparent quenching constants K_{SV} and $(\text{PRU}/Q)_{50}$ are given in ref 4. In the case of nonstoichiometric quenching, one can estimate the quenching volume in the microphase as $V_{Qm} \approx K_{Qm}$, which occurs to be about 0.3 of the total volume of polymer molecule (Figure 4).

According to the microphase model the dependence of K_{SV} on $[\text{PRU}]_0$ is caused by the dependence of the local concentration of the quencher in the microphase $[Q]_{0m}$ on $[\text{PRU}]_0$

$$[Q]_{0m} \approx \frac{[Q]_0}{v_m} = \frac{1000[Q]_0}{M_{\text{PRU}}[\text{PRU}]_0} \quad (12)$$

where $v_m \approx M_{\text{PRU}}[\text{PRU}]/1000$ is a relative volume of the microphase and M_{PRU} is a molecular mass of PRU, and $(\text{PRU}/Q)_{50}$ does not depend on $[\text{PRU}]_0$

$$\left(\frac{\text{PRU}}{Q}\right)_{50} = \frac{[\text{PRU}]_0}{[Q]_{1/2}} = \frac{1000K_{Qm}}{M_{\text{PRU}}} \quad (13)$$

Concentration of the luminescent centers in the microphase does not depend on the concentration of microphase and is equal to $[L]_{m0} = \beta 1000/M_{\text{PRU}}$, where β is an actual fraction of emitting centers per each polymer repeat unit (light absorbing center). Total concentration of these luminescent centers in the solution is $[L]_0 = \beta[\text{PRU}]_0$. In the case of the stoichiometric complex formation the dependence of the luminescence quantum yield on the total quencher concentration can be expressed as

$$\begin{aligned} \frac{\phi}{\phi_0} = \frac{[L]_m}{[L]_{m0}} &= 1 - \frac{1 + \frac{1}{K_{Cm}[L]_{m0}} + \frac{[Q]_{m0}}{[L]_{m0}}}{2} \\ &+ \left(\frac{\left(1 + \frac{1}{K_{Cm}[L]_{m0}} + \frac{[Q]_{m0}}{[L]_{m0}}\right)^2}{4} - \frac{[Q]_{m0}}{[L]_{m0}} \right)^{1/2} \\ &= 1 - \frac{1 + \frac{1}{K_Q\beta[\text{PRU}]_0} + \frac{[Q]_0}{\beta[\text{PRU}]_0\left(v_m + \frac{1}{\rho_Q}\right)}}{2} \\ &+ \left(\frac{\left(1 + \frac{1}{K_Q\beta[\text{PRU}]_0} + \frac{[Q]_0}{\beta[\text{PRU}]_0\left(v_m + \frac{1}{\rho_Q}\right)}\right)^2}{4} \right. \\ &\quad \left. - \frac{[Q]_0}{\beta[\text{PRU}]_0\left(v_m + \frac{1}{\rho_Q}\right)} \right)^{1/2} \end{aligned} \quad (14)$$

At small $[Q]_{0m} < [L]_{0m}$, ratio ϕ_0/ϕ follows the Stern–Volmer equation and one can estimate $[L]_0 \approx 1/K_{SV}$ and $[L]_{0m} \approx 1/v_m K_{SV}$ (the latter does not depend on $[\text{PRU}]$). The obtained values of $1/[L]_{0m}$ were found to depend linearly on n_{PRU} with the slope ~ 0.3 at $n_{\text{PRU}} < 200$ and reaches the limit $[L]_{0m} = 0.008 \text{ molec}/\text{nm}^3$ at $n_{\text{PRU}} > 200$ (Figure 4). A value of β decreases from 0.2 to 0.01, when n_{PRU} increases from 33 to 250. The efficiency of quenching rises with the increase of the size of the polypeptide molecule and K_{Qm} corresponds ca. one-third of the polymer molecule volume (equal to ca. $1.3n_{\text{PRU}} \text{ nm}^3$). This indicates that excitation can migrate through ca. 200 residues of the dye, connected with the polypeptide chain ($l \sim 100 \text{ nm}$) to reach a quencher molecule.

Quenching of Fluorescence of Polyfluorene-phenylene by Au_n Nanoparticles. Extremely efficient super-quenching by Au_n nanoparticles with various diameters (2–20 nm) was observed for luminescence of conjugated cationic polymer poly(9,9-bis(6-*N,N,N*-trimethylammonium)-hexyl)-fluorene-phenylene (PF) in aqueous solutions.¹⁰ In this case, luminescence quenching is observed at very low concentrations of nanoparticles ($\sim 10 \text{ pM}$) and $(\text{PRU}/Q)_{50}$ reaches 85 000. Estimation of $([Q]/[\text{Polymer}])_{1/2}$ by eq 11 indicates that one nanoparticle can quench luminescence of ~ 4000 polymer molecules. This suggests very strong association of cationic polymer molecules in microphase, which constitute some kind of large micelles (with radius $\sim 100 \text{ nm}$). In the absence of this association average distance between polymer molecules in the solution ($[\text{PRU}]_0 = 1 \text{ }\mu\text{M}$) would be too large ($> 100 \text{ nm}$) for any mechanism of radiationless energy transfer. The increase of ionic strength causes a strong decrease of quenching.¹⁰ This decrease can be attributed to the destruction of these associates at high ionic strength and disappearance of the conditions for

efficient energy migration. This effect provides an additional argument for association of the polymer molecules.

The plot of $\ln(\varphi/\varphi_0)$ versus $[Q]_0$ is close to linear with the slope 0.05 pM^{-1} , which can indicate the nonstoichiometric interaction with $V_{Qm} = 4 \times 10^6 \text{ nm}^3/\text{molecule}$ (Figure 5). But the initial slope of this plot (at $[Q]_0 < 20 \text{ pM}$) is some greater ($V_{Qm} \approx 7 \times 10^6 \text{ nm}^3/\text{molecule}$) and this part of the plot φ/φ_0 versus $[Q]_0$ can be approximated better by eq 6, corresponding to the stoichiometric complex formation with $K_Q = 0.27 \text{ pM}^{-1}$ and very small ($\sim 10^{-5}[\text{PRU}]_0$) apparent concentration of the emitting centers ($\beta[\text{PRU}]_0 = 12 \text{ pM}$). This feature of the dependence φ/φ_0 versus $[Q]_0$ can indicate that an infinite series of complexes LQ_n with equal equilibrium constants can be formed and these equilibrium constants are some smaller than that for the first complex LQ $V_{Qm} < K_{Qm}$ (see Table 2). On this reason the dependence φ/φ_0 on $[Q]_0$, corresponding to the formation of complex LQ (eq 6) dominates at small $[Q]_0$ ($< 0.2 \text{ }\mu\text{M}$) and the Perrin dependence starts to dominate at higher $[Q]_0$. In any case strong association ($\sim 10^4$) of the polymer molecules is required to provide an efficient energy transfer in compact aggregates. Fast energy transfer in so large J-aggregates ($\sim 10^4$ monomer units) is known to occur for instance in Langmuir–Blodgett films.^{32,33} Thus, the aggregation of polyelectrolyte molecules, which promotes energy migration can provide additional amplification of the superquenching.

CONCLUSIONS

The phenomenon of superquenching, observed in the solutions of polyelectrolytes can be treated as a formation of the microphase, where the local concentrations of the solubilized reactants exceed their apparent concentrations in the solution 10^4 – 10^6 times. The increase of the local concentrations is responsible for the enhanced values of apparent quenching constants, which exceed the actual quenching constants in the microphase, related to the formation of nonluminescent complexes 10^4 – 10^6 times. Additional amplification ($\sim 10^2$ – 10^5 times) can be provided by auspicious conditions for formation of aggregates of light absorbing centers, where efficient energy transfer can occur.

The observed dependence of the fluorescence quantum yield on quencher concentration indicates the formation of rather weak complexes LQ with $K_{LQm} \sim 10^2 \text{ M}^{-1}$ and $\Delta G_{LQm} \approx -0.2 \text{ eV}$ in microphase. Formation of a series of nonfluorescent complexes LQ_n ($n > 1$) with equilibrium constants 5–10 times smaller than that for the first complex, or some nonstoichiometric quenching with apparent radius $R_Q \sim 1$ – 4 nm are possible at greater concentrations of the quencher. One can expect the formation of several microphases (related, for instance, to the intercalation of the dye molecule between DNA bases and partly to the deposition of the dye on the DNA minor groove, which contributes to electrostatic interaction between the positively charged dye and the negatively charged phosphate groups of DNA molecule³⁰) with some different properties (K_{LQm} , ρ_{QD} , v_{mi}) for these polyelectrolytes, but real accuracy and reproducibility of the experimental data do not allow to separate these parameters for several microphases in the general case. In all the examples considered, no strong and specific interactions between the luminescent centers and a quencher in the microphase were observed. The whole specificity of the luminescent sensors, using superquenching is based on the specificity of the binding of definite quencher (analyte) by the polypeptides (surfactant). Formation of large

associates of polymer molecules, containing luminescent centers (up to 10^4 molecules and radius $\sim 100 \text{ nm}$) observed for poly(9,9-bis(6-*N,N,N*-trimethylammonium)-hexyl)-fluorene phenylene provides the conditions for a very efficient energy transfer inside these associates and very strong amplification of the quenching.

Original idea to use simultaneously two different kinds of probes, Au_n nanoparticles (which can be studied by electron and tunnel microscopy) and luminescent probes (which can be studied by optical methods) for investigation of the structure of DNA molecules, unfortunately fails because these probes have different and nonspecific localization in DNA molecules. Nevertheless, microphase approach provides interesting new possibilities for analysis and control of kinetics of various important DNA reactions in native media (including the damage and replication of DNA). Even at small apparent concentrations of the reactants in the cell their local concentrations in the microphase of DNA occur to be several orders of magnitude ($\sim 10^5$ – 10^8) higher and sufficient for fast interaction. Besides, this approach provides new opportunities for improvement of various sensors, using simple method of extraction by microphase, formed by various surfactants, added to the sample, and excluding additional procedures of the separation.

AUTHOR INFORMATION

Corresponding Authors

*E-mail: (M.G.K.) kuzmin@photo.chem.msu.ru.

*E-mail: (V.A.K.) vak@sky.chph.ras.ru.

Notes

The authors declare no competing financial interest.

REFERENCES

- (1) Chen, L.; McBranch, D. W.; Wang, H.; Helgeson, R.; Wudl, F.; Whitten, D. G. Highly Sensitive Biological and Chemical Sensors Based on Reversible Fluorescence Quenching in a Conjugated Polymer. *Proc. Natl. Acad. Sci. U.S.A.* **1999**, *96*, 12287–12292.
- (2) Heeger, P. S.; Heeger, A. J. Making Sense of Polymer-Based Biosensors. *Proc. Natl. Acad. Sci. U.S.A.* **1999**, *96*, 12219–12221.
- (3) Jones, R. M.; Lu, L.; Helgeson, R.; Bergstedt, T. S.; McBranch, D. W.; Whitten, D. G. Building Highly Sensitive Dye Assemblies for Biosensing from Molecular Building Blocks. *Proc. Natl. Acad. Sci. U.S.A.* **2001**, *98*, 14769–14772.
- (4) Lu, L.; Helgeson, R.; Jones, R. M.; McBranch, D.; Whitten, D. Superquenching in Cyanine Pendant Poly(l-lysine) Dyes: Dependence on Molecular Weight, Solvent, and Aggregation. *J. Am. Chem. Soc.* **2002**, *124*, 483–488.
- (5) Gaylord, B. S.; Heeger, A. J.; Bazan, G. C. DNA Detection Using Water-Soluble Conjugated Polymers and Peptide Nucleic Acid Probes. *Proc. Natl. Acad. Sci. U.S.A.* **2002**, *99*, 10954–10957.
- (6) Wang, D.; Gong, X.; Heeger, P. S.; Rininsland, F.; Bazan, G. C.; Heeger, A. J. Biosensors from Conjugated Polyelectrolyte Complexes. *Proc. Natl. Acad. Sci. U.S.A.* **2002**, *99*, 49–53.
- (7) Fan, C.; Plaxco, K. W.; Heeger, A. J. High-Efficiency Fluorescence Quenching of Conjugated Polymers by Proteins. *J. Am. Chem. Soc.* **2002**, *124*, 5642–5643.
- (8) Swager, T. M. The Molecular Wire Approach to Sensory Signal Amplification. *Acc. Chem. Res.* **1998**, *31*, 201–207.
- (9) Swager, T. M.; Wosnick, J. H. Self-Amplifying Semiconducting Polymers for Chemical Sensors. *MRS Bull.* **2002**, *27*, 446–450.
- (10) Fan, C.; Wang, S.; Hong, J. W.; Bazan, G. C.; Plaxco, K. W.; Heeger, A. J. Beyond Superquenching: Hyper-Efficient Energy Transfer from Conjugated Polymers to Gold Nanoparticles. *Proc. Natl. Acad. Sci. U.S.A.* **2003**, *100*, 6297–6301.

- (11) Kumaraswamy, S.; Bergstedt, T.; Shi, X.; Rininsland, F.; Kushon, S.; Xia, W.; Ley, K.; Achyuthan, K.; McBranch, D.; Whitten, D. Fluorescent-Conjugated Polymer Superquenching Facilitates Highly Sensitive Detection of Proteases. *Proc. Natl. Acad. Sci. U.S.A.* **2004**, *101*, 7511–7515.
- (12) Rininsland, F.; Xia, W.; Wittenburg, S.; Shi, X.; Stankewicz, C.; Achyuthan, K.; McBranch, D.; Whitten, D. Metal Ion-Mediated Polymer Superquenching for Highly Sensitive Detection of Kinase and Phosphatase Activities. *Proc. Natl. Acad. Sci. U.S.A.* **2004**, *101*, 15295–15300.
- (13) Jones, R. M.; Kumaraswamy, S.; Lu, L.; Rininsland, F.; Ley, K.; Xia, W.; McBranch, D.; Whitten, D. G. Fluorescent Polymer Superquenching-Based Bioassays. Patent application number: 20080213747, Publication date: 09/04/2008.
- (14) Lisitsyna, E. S.; Lygo, O. N.; Durandin, N. A.; Dementieva, O. V.; Rudoy, V. M.; Kuzmin, V. A. Superquenching of SYBRGreen Dye Fluorescence in Complex with DNA by Gold Nanoparticles. *High Energy Chem.* **2012**, *46*, 363–367.
- (15) Gehlen, M. H.; De Schryver, F. C. Time-Resolved Fluorescence Quenching in Micellar Assemblies. *Chem. Rev.* **1993**, *93*, 189–221.
- (16) Fendler, J. H. Interactions and Reactions in Reversed Micellar Systems. *Acc. Chem. Res.* **1976**, *9*, 153–161.
- (17) Berezin, I. V.; Martinek, K.; Yatsimirskii, A. K. Physicochemical Foundations of Micellar Catalysis. *Russ. Chem. Rev.* **1973**, *42*, 787–833.
- (18) Martinek, K.; Levashov, A. V.; Klyachko, N. L.; Khmelnitsky, Yu. L.; Berezin, I. V. Micellar Enzymology. *Eur. J. Biochem.* **1986**, *155*, 453–468.
- (19) Soboleva, I. V.; Kuzmin, M. G. Kinetic Patterns of Electron Phototransfer Reactions in Micellar Systems. Quenching of Ru-(bipy)²⁺₃ Luminescence by Electron Acceptors. *Russ. J. Phys. Chem.* **1994**, *68*, 282–289.
- (20) Kuzmin, M. G.; Soboleva, I. V. Kinetic Patterns of Electron Phototransfer Reactions in Micellar Systems. The Influence of Solubilization on the Redox Properties of Reagents. *Russ. J. Phys. Chem.* **1994**, *68*, 290–295.
- (21) Soboleva, I. V.; van Stam, J.; Dutt, G. B.; Kuzmin, M. G.; De Schryver, F. Electron-Transfer Reactions in SDS Micelles: Reactivity of Pyrene and Tris(2,2'-bipyridyl)ruthenium(II) Excited States Investigated by Time-Resolved Luminescence Quenching. *Langmuir* **1999**, *15*, 6201–6207.
- (22) Kuzmin, M. G.; Soboleva, I. V.; Kotov, N. A. Kinetics of Photoinduced Charge Transfer at Microscopic and Macroscopic Interface. *Anal. Sci.* **1990**, *15*, 3–16.
- (23) Soboleva, I. V.; Kuzmin, M. G. The Pseudophase and Compartmental Kinetic Models of Photoreactions in Micelles. *Russian J. Phys. Chem. A* **2000**, *74*, 1569–1578.
- (24) Nikiforova, E. M.; Bryleva, E. Yu.; Mchedlov-Petrosyan, N. O. The Distribution of the Anion Zwitterionforms of Methyl Orange between the Dispers Microemulsion Pseudophase and Continuous Water Phase. *Russian J. Phys. Chem. A* **2008**, *82* (9), 1434–1437.
- (25) Sambrook, J.; Fritsch, E. F.; Maniatis, T. *Molecular Cloning: A Laboratory Manual*; Cold Spring Harbor Laboratory Press: New York, 1989.
- (26) Zipper, H.; Brunner, H.; Bernhagen, J.; Vitzthum, F. Investigations on DNA Intercalation and Surface Binding by SYBR Green I, Its Structure Determination and Methodological Implications. *Nucleic Acids Res.* **2004**, e103.
- (27) Duff, D. G.; Baiker, A.; Edwards, P. P. A New Hydrosol of Gold Clusters. 1. Formation and Particle Size Variation. *Langmuir* **1993**, *9*, 2301–2309.
- (28) Giglio, S.; Monis, P. T.; Saint, C. P. Demonstration of Preferential Binding of SYBR Green I to Specific DNA Fragments in Real-Time Multiplex PCR. *Nucleic Acids Res.* **2003**, *31* (22), e136.
- (29) Dragan, A. I.; Pavlovic, R.; McGivney, J. B.; Casas-Finet, J. R.; Bishop, E. S.; Strouse, R. J.; Schenerman, M. A.; Geddes, C. D. SYBR Green I: Fluorescence Properties and Interaction with DNA. *J. Fluoresc.* **2012**, *22* (4), 1189–99.
- (30) Xu, Q.; Liu, J.; He, Zh.; Yang, S. Superquenching Acridinium Ester Chemiluminescence by Gold Nanoparticles for DNA Detection. *Chem. Commun.* **2010**, *46*, 8800–8802.
- (31) Scatchard, G. The Attraction of Proteins for Small Molecules and Ions. *Ann. N.Y. Acad. Sci.* **1949**, *51*, 660–672.
- (32) Chromophore coupling effects. In *J-Aggregates*; Kobayashi, T., Ed; World Scientific: Singapore, 1996, 1–40.
- (33) Moebius, D.; Kuhn, H. Energy transfer in monolayers with cyanine dye Sheibe aggregates. *J. Appl. Phys.* **1988**, *64*, 5138–5144.